Structural characterization and plasmonic properties of two-dimensional arrays of hydrophobic large gold nanoparticles fabricated by Langmuir-Blodgett technique

Ishida, Takuya
Department of Materials Physics and Chemistry, Graduate School of Engineering, Kyushu University

Tachikiri, Yuki
Department of Materials Physics and Chemistry, Graduate School of Engineering, Kyushu University

Sako, Takayuki
Department of Materials Physics and Chemistry, Graduate School of Engineering, Kyushu University

Takahashi, Yukina
Department of Applied Chemistry, Faculty of Engineering, Kyushu University

他

出版情報：Applied Surface Science. 404, pp.350-356, 2017-05. Elsevier
バージョン：
権利関係：

Structural Characterization and Plasmonic Properties of Two-Dimensional Arrays of Hydrophobic Large Gold Nanoparticles Fabricated by Langmuir-Blodgett Technique

Takuya Ishida[†], *Yuki Tachikiri*[†], *Takayuki Sako*[†], *Yukina Takahashi*[*,‡], *Sunao Yamada*[*,‡,§]

[†]Department of Materials Physics and Chemistry, Graduate School of Engineering, Kyushu University, 744 Moto-oka, Nishi-ku, Fukuoka 819-0395, Japan

[‡]Department of Applied Chemistry, Faculty of Engineering, Kyushu University, 744 Moto-oka, Nishi-ku, Fukuoka 819-0395, Japan

[§]Center for Future Chemistry, Kyushu University, 744 Moto-oka, Nishi-ku, Fukuoka 819-0395, Japan

KEYWORDS Localized surface plasmon, Two-dimensional array, Hydrophobic gold nanoparticles, Langmuir-Blodgett

ABSTRACT

We have succeeded in fabricating two-dimensional (2D) arrays of larger gold nanoparticles (AuNPs) (diameters 17, 28, and 48 nm) by Langmuir-Blodgett (LB) method. Although the particle size of AuNPs is one of the most important factors in order to control the optical properties of 2D arrays, there have been reported only the size of less than ~20 nm. This is a first report on the bottom-up fabrication of 2D arrays consisting of hydrophobic AuNP with the diameter of ~50 nm, of which the size is expected to obtain maximum near-field effects. Octadecylthiolate-capped AuNPs (ODT-AuNPs) which were prepared by our method could be re-dispersed in chloroform even after drying completely, realizing the spreading of the colloidal chloroform solution onto the water surface. Accordingly, densely-packed 2D LB films of ODT-AuNPs could be fabricated on an indium-tin-oxide substrate, when water as the subphase and polyethylene glycol (PEG) as an amphiphilic agent were used. PEG played an important role to form densely-packed film uniformly due to increasing affinity between hydrophobic AuNP and water. Absorption spectra of the films revealed that the resonance wavelengths of plasmon oscillation through interparticle plasmon coupling were clearly correlated with the particle sizes rather than deposition densities.

1. Introduction

In recent years, plasmonics as a new technology which can confine electromagnetic fields in nanoscale space, using plasmonic nanoparticles and/or nanostructures, has attracted much attention for breaking diffraction limit of light field.[1,2] It is due to the fact that localized surface plasmon resonance (LSPR) of metal nanoparticles can be excited directly with incident light.[3] In addition, LSPR generates enhanced electromagnetic fields in the vicinity of the metal surface.[3,4] The enhanced fields were utilized for the improvement of the efficiencies of molecular photoexcitation,[5-7] fluorescence,[5-9] and photoelectric conversion[7,10-

[17] at the surface vicinities of metal nanoparticle. Furthermore, LSPR can be applied for the detection of local refractive index change at the surface region of metal nanoparticles, utilized as LSPR sensors.[18-20] Among the plasmonic nanoparticles, gold nanoparticles (AuNPs) were especially attractive nanomaterials because they possess excellent chemical stability, low toxicity to biological tissues,[21-23] and their surfaces can be easily modified with organic compounds such as thiols.[24-29] Accordingly, they are expected for various applications such as solar cells,[16,17,30-32] emission devices,[33-35] sensors,[18-20] biological and medical probes,[21-23,36] and so on. The field enhancement and the resonant wavelength of spherical AuNPs by LSPR is generally observed around 520-560 nm region, and the maximum field enhancement caused by LSPR is achieved for diameters of around 50 nm.[4]

On the other hand, collective LSPR[37] among AuNPs are generated by interparticle plasmon coupling when they are properly arranged with appropriate spatial distances. As to the fabrication method of plasmonic two-dimensional (2D) gold nanostructures, dry processes such as electron beam lithography[38,39] and vapor deposition[34,40] are well known methods. However, they are inadequate for the large scale preparation of 2D array, because of time and cost consuming for fabrication. Thus, 2D arrays of AuNPs, fabricated by wet processes, have been receiving considerable attention because the collective LSPR can be directly excited by the incident light and can be propagated in the wide area of 2D arrays. In addition, they are expected to generate much stronger enhanced fields in the void of 2D arrays than corresponding single AuNP, so that they can also be applied to multiphoton-excited reactions with incoherent light in the region of visible to near IR.[38,41,42] There are several approaches of wet processes to fabricate 2D arrays of AuNPs such as electrostatic adsorption,[7,43,44] electrophoretic deposition,[45] liquid films using liquid-liquid interface,[27,46-48] Langmuir-Blodgett (LB) technique[37,49-55] are also reported. Among them, the LB technique is especially superior to the others for controlling the density of 2D arrays in wide area. For

example, controlling the resonant wavelength by changing the interparticle distance among plasmonic nanoparticles in the 2D arrays[37] or laminating the 2D arrays[56,57] has been reported. Alternatively, changing the diameters of AuNPs is a potential candidate for controlling the resonant wavelength and the strength of the field. However, as far as we know, 2D arrays of AuNPs fabricated by using LB technique have been limited up to ~20 nm diameters. It was caused by that satisfactorily methods of preparing hydrophobic and highly-dispersing AuNPs with larger diameters, and of fabricating their densely-packed arrays by means of LB method have not yet been developed.

In order to solve the first problem concerning the hydrophobic AuNPs, we recently have reported the very simple method of preparing hydrophobic octadecylthiolate (ODT) - protected AuNPs with larger sizes (diameter: 17-48 nm) which were also stable in the solid state and could be re-dispersed in chloroform, by using ethanol solution of octadecanethiol, and subsequent extraction with chloroform.[29] The second problem as for LB film formation of lager AuNPs is due to stronger van der Waals interaction causing aggregation and agglomeration. Actually, it is difficult to fabricate densely-packed film uniformly owing to the formation of agglomeration.[53] It was reported that fabrication of densely-packed film consisting of hydrophobic nanoparticles had been achieved by the decrease of hydrophobic interactions using other subphase, such as ethylene glycol (EG) and diethylene glycol (DEG)[53] having higher affinity for hydrophobic AuNPs than water, or surfactants[54,55] increasing the affinity between the AuNPs and water. In this study, we have successfully fabricated 2D arrays of ODT-AuNP films with larger diameters (17-48 nm) on an indium-tin-oxide (ITO) substrate by using the LB method with polyethylene glycol (PEG), and found that the resonant wavelengths of collective LSPR were clearly correlated with the size rather than the density of deposited AuNPs.

2. Experimental Section

All starting materials were commercially purchased and used without further purification. Milli-Q water with the resistivity of 18.2 MΩ cm was used throughout the experiments. Citrate-protected AuNPs (cit-AuNPs) were prepared by using citrate ion as a reducing reagent. Namely, a solution of $HAuCl_4$ (0.010 wt% in Milli-Q water, 300 mL) was heated to the boiling temperature. Then, an aqueous solution of sodium citrate (1.0 wt%, 7.5, 3.7 or 2.4 mL) was added to the boiling solution of $HAuCl_4$, giving cit-AuNPs (cit-AuNP/water) with the diameter of 17, 28 or 48 nm, respectively. The reaction mixture was kept at the boiling temperature for 60 min, and was allowed to cool down to room temperature. Next, hydrophobic AuNP was prepared from cit-AuNPs by a ligand-exchange process. First, 800 mg of octadecanethiol (ODT) was dissolved into 20 mL of ethanol by ultrasonic irradiation for 10 min. Subsequently, the colloidal solution (20 mL) of as-prepared cit-AuNPs with the diameter of 17, 28 or 48 nm was added to the ethanol solution of ODT under vigorous stirring for 24 h. Then, chloroform (5 mL) was added to the reaction mixture followed by sonication, in order to extract the resultant AuNPs capped with ODT (ODT-AuNPs).[29] Then, the organic phase was centrifuged so as to remove excess ODT (12,000 x g, 10 min, 5 times). The ODT-AuNPs were obtained as powder state after vacuum drying. A noteworthy characteristics of obtained ODT-AuNPs was that they were re-dispersed into chloroform.

ODT-AuNP films were fabricated by the LB technique. First, dried ODT-AuNPs (5.0 mg) were re-dispersed into chloroform (1.0 mL) with or without PEG of 50 ng mL^{-1} by sonication. PEG was used as an amphiphilic polymer which helped to spread the hydrophobic AuNPs onto water and to form uniform AuNP monolayer. Then, 200 μL solution of ODT-AuNP with or without PEG was spread on the surface of water as the

subphase in the LB trough (USI-3-22QY, USI, Japan) at 25℃, and kept for 15 min to evaporate the solvent. The resultant nanoparticle film was compressed at a speed of 0.1 mm s^{-1}, and then transferred onto an ITO substrate by LB method at a speed of 0.2 mm s^{-1}. The ITO substrate was beforehand cleaned by ultrasonication in water and acetone for 5 min, followed by cleaning with UV-ozone for 15 min and subsequent immersion into the boiling 2-propanol for 10 min. It was dried with nitrogen gas just before use. UV-vis spectra were recorded on JASCO V-670ST. Scanning electron microscopy (SEM) and transmission electron microscopy (TEM) were performed on Hitachi SU-8000 and JEOL JEM-200CX, respectively.

3. Results and Discussion

We previously reported that it was successful to prepare relatively large hydrophobic AuNPs (d = 17-48 nm) which exhibited distinct LSPR and could be dispersed into chloroform.[29] Figure 1 shows extinction spectra of ODT-AuNP/$CHCl_3$ before and after drying process and cit-AuNP/water with different sizes. Distinct spectral red-shift of the extinction peaks with increasing the particle size, as well as reasonable spectral shift due to the change of refractive index in the vicinity of the AuNP surface by the ligands and solvent were observed. Namely, the extinction peak of the AuNPs with the diameter of 17 ± 2, 28 ± 7, and 48 ± 7 nm (Figure S1) were shifted from 519, 529, and 533 nm to 533, 540, and 543 nm, respectively. As novel revelation in this study, we found that the spectra of ODT-AuNP/$CHCl_3$ before and after drying showed no appreciable changes, as can be recognized from Figure 1. To the best of our knowledge, there are no reports of such very stable yet hydrophobic large AuNPs with the diameter of as large as ~50 nm.

Then, the LB films of ODT-AuNPs were fabricated, where water was used as the subphase. Figure 2 shows surface pressure-area (π-A) isotherm of ODT-AuNP (d = 17 nm) with and without PEG, and surface elastic modulus (K_s), which reflected the state of Langmuir film (L film) at an air-water interface, was calculated as

$$K_s = -A\left(\frac{d\pi}{dA}\right) \quad (1)$$

where π and A are the surface pressure and surface area, respectively. V. Aleksandrovic *et al.* [53] reported that ethylene glycol (EG) and diethylene glycol (DEG), which exhibit higher affinity for hydrophobic nanoparticles than water, were employed as subphases so as to spread onto organic solvent-air interface and to form a densely-packed monolayer film. Furthermore, C. Y. Law *et al.* [54] reported that excess amphiphilic molecules enabled hydrophobic AuNPs to form a densely-packed monolayer film on water-air interface. Hence, PEG was expected to exhibit similar effects to EG and DEG as an amphiphilic polymer. Also, we have optimized the amount of PEG resulted in 50 ng mL^{-1} indicating the maximum absorption peak (see Supporting Information S3). Namely, this result implies that the fabricated substrate in the present condition has the highest coverage of the AuNPs. In Figure 2, solid and dashed lines show the π-A isotherm and the surface elasticity of the 2D arrays of 17 nm AuNPs formed at the water surface, respectively. In spite of the absence and the presence of PEG, the surface pressure increased gently in the region of 400-800 nm^2 $AuNP^{-1}$ and then-sharply in the region of 200-400 nm^2 $AuNP^{-1}$. But the presence of PEG showed higher surface pressure and elasticity, suggesting the formation of more stable and larger L film.

Figure 3 shows SEM images of LB films fabricated on ITO substrates. In the absence of PEG, some disk-like domains (islands)[51,58] consisting of the ODT-AuNPs were formed and the distances among the domains decreased with proceeding compression from 7 to 14 mN m^{-1} (Figure 2 a, 3 a1, and 3 a2) by collision and coalescence of the domains.[59] The coalescence of domains which allowed further compression and generated higher dense LB films at 25 mN m^{-1} (Figure 3 a3). As was recognized from Figure 2 a, π-A isotherms where the surface pressure increased rapidly in the region of 200-400 nm^2 $AuNP^{-1}$ (in the region of 10 to 30 mN m^{-1}) indicated proceeding of collision and coalescence[59,60]. Some of the ODT-AuNP layers were observed to be piled up, or collapsed at 38 mN m^{-1}, in spite of remaining free spaces (Figure 3 a4). In the presence of PEG, the distances among the domains also decreased with proceeding compression by collision and coalescence of the domains, from 7 to 14 mN m^{-1} (Figure 2 b, 3 b1, and b2). However, remarkable coalescence of domains forming densely packed 2D arrays was clearly observed with larger areas without appreciable collapsing at 25 and 38 mN m^{-1} (Figure 3 b3 and b4), respectively, as compared with the case of the absence of PEG. Furthermore, the densely-packed uniform 2D array without free space could be formed with a remarkably larger area at 45 mN m^{-1} (Figure 3 b5). Fast Fourier transfer (FFT) images of the 2D array formed at 45 mN m^{-1} (Figure S4) support that the reultant 2D film has a densely-packed, hexagonal, and periodic structure. The results of the π-A isotherms in the absence and the presence of PEG also shows that PEG affects the coalescence of domains leading uniform L film with larger area, especially at higher surface pressures. The limiting surface pressure before collapsing was ~40 mN m^{-1} in the absence of PEG, while ~50 mN m^{-1} in the presence of PEG. Furthermore, in the presence of PEG, the slope of the π-A isotherm increased again during 40-50 mN m^{-1}, so that PEG assisted the formation of highly-ordered 2D array formation ODT-AuNPs.[53,61] These results can be explained that PEG decreased the interfacial tension between AuNPs and water resulted in

uniform 2D array. The hydrophobic interaction could be a main driving force for the formation of domains composed of hydrophobic AuNPs. As an amphiphilic agent on domain-water interface, PEG enabled rearrangement of the domains because the hydrophobic interaction around AuNPs correlated with the stability and the rigidity of the domains. In fact, in the absence of PEG, the domains of the AuNPs could not transform uniform and densely-packed AuNP monolayer with compression because of the inflexibility due to the hydrophobic interaction with ODT. In the presence of PEG, on the other hand, the domains of AuNPs could transform to the uniform array through transitional state in which some domains were coalesced into a new domain with larger area.

Figure 4 shows the extinction spectra of the ODT-AuNP films on ITO substrates without and with PEG, respectively. The red-shift of the peak to ~610 nm, as compared with the case of the colloidal solution (Figure 1), was observed due to interparticle plasmon coupling.[37,62] Slight fluctuation of peaks was unavoidable. Also, the extinction intensity increased with increasing the surface pressure. In both cases, somewhat peak shifts at 3 mN m^{-1} were observed, though the reason is not clear at this stage. The extinction and the coverage were largest at 45 mN m^{-1} in the presence of PEG. These results are consistent with the SEM observations that the coverage of ODT-AuNPs increased with increasing the surface pressure (Figure S5). However, the peak position of the AuNP film was not necessarily correlated with the surface pressure, implying no appreciable correlations between the surface pressures and particle distances as well as the distances among the domains. The AuNP densities in the domains were found to be independent of the surface pressure, as confirmed from the SEM images.

Fabrication of 2D arrays of larger ODT-AuNPs (d = 28 and 48 nm) were also examined by using PEG. Figure 5 shows π-A isotherms of the AuNPs, showing L films as in the case of

AuNPs (d = 17 nm). In both cases, surface pressures increases above 30 mN m^{-1}, indicating the formation of L films. Then, the L films of both ODT-AuNPs were transferred to the ITO substrate at 36 and 31 mN m^{-1}, respectively. Figure 6 shows SEM images of the LB films. In both sizes of AuNPs, formation of densely-packed 2D arrays of the ODT-AuNPs was clearly obserbed. Figure 7 shows the extinction spectra of the fabricated LB films of the three different sizes of ODT-AuNPs. The peak wavelengths of 17, 28, and 48 nm AuNPs were observed at 609, 636, and 691 nm, respectively. Clearly, it shifted to longer wavelength with increasing the particle size, and also showed red-shifts than those of the corresponding ODT-AuNPs in the colloidal solutions of chloroform. Accordingly, the resonant wavelength could be controlled by changing the particle size rather than the deposited density of ODT-AuNP, by using PEG. As far as we know, this is a first report on the bottom-up fabrication of hydrophobic AuNP with as large as ~50 nm, by using the LB method.

CONCLUSIONS

We have succeeded in fabricating 2D arrays of larger-size AuNPs (d = 17, 28 or 48 nm) that were hydrophobized with ODT through the simple two-step procedure using ethanol as an amphiphilic solvent, and subsequent transformation of the L films with the assistance of PEG at the water surface fabricated the LB films on ITO substrates. The resonant wavelengths of the 2D arrays could be controlled by changing the particle size rather than changing the deposition density. The noteworthy advantage of the present method is that the as-prepared ODT-AuNPs were stable in the dried state, and subsequent re-dispersion was possible in chloroform, in spite of such large sizes, resulting the realization of 2D arrays using the LB method. Since the strength of LSPR was largest where AuNPs were around 50

nm size, the present results open up further applications of large plasmonic nanoparticles in various fields.

FIGURES

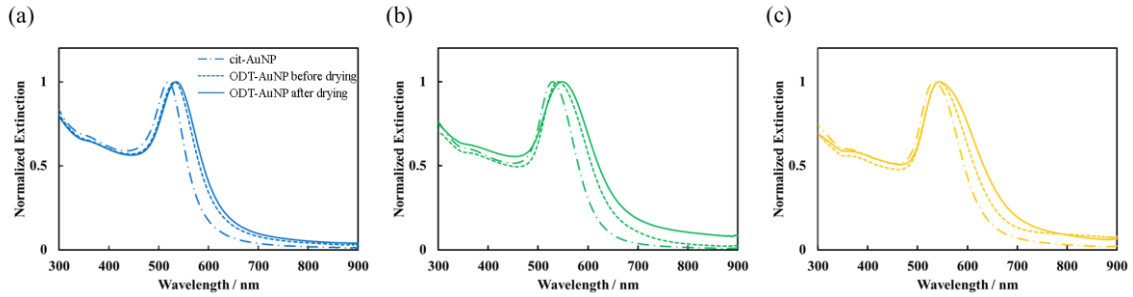

Figure 1. Extinction spectra of cit-AuNP/water (chain line), ODT-AuNP/$CHCl_3$ before (dashed line) and after drying (solid line) with the diameter of (a) 17, (b) 28, and (c) 48 nm.

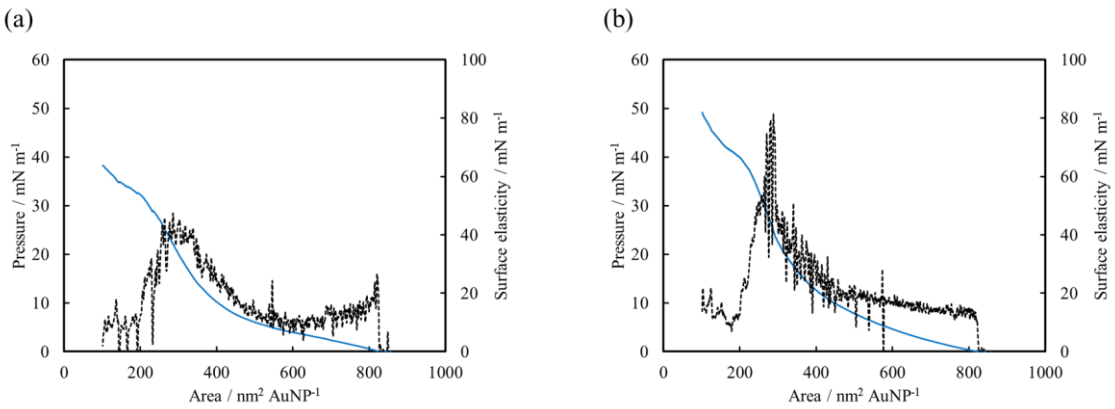

Figure 2. Surface pressure (π)-Area (A) isotherm (solid line) and surface elasticity (dashed line) of ODT-AuNP (d = 17 nm) (a) without PEG and (b) with PEG.

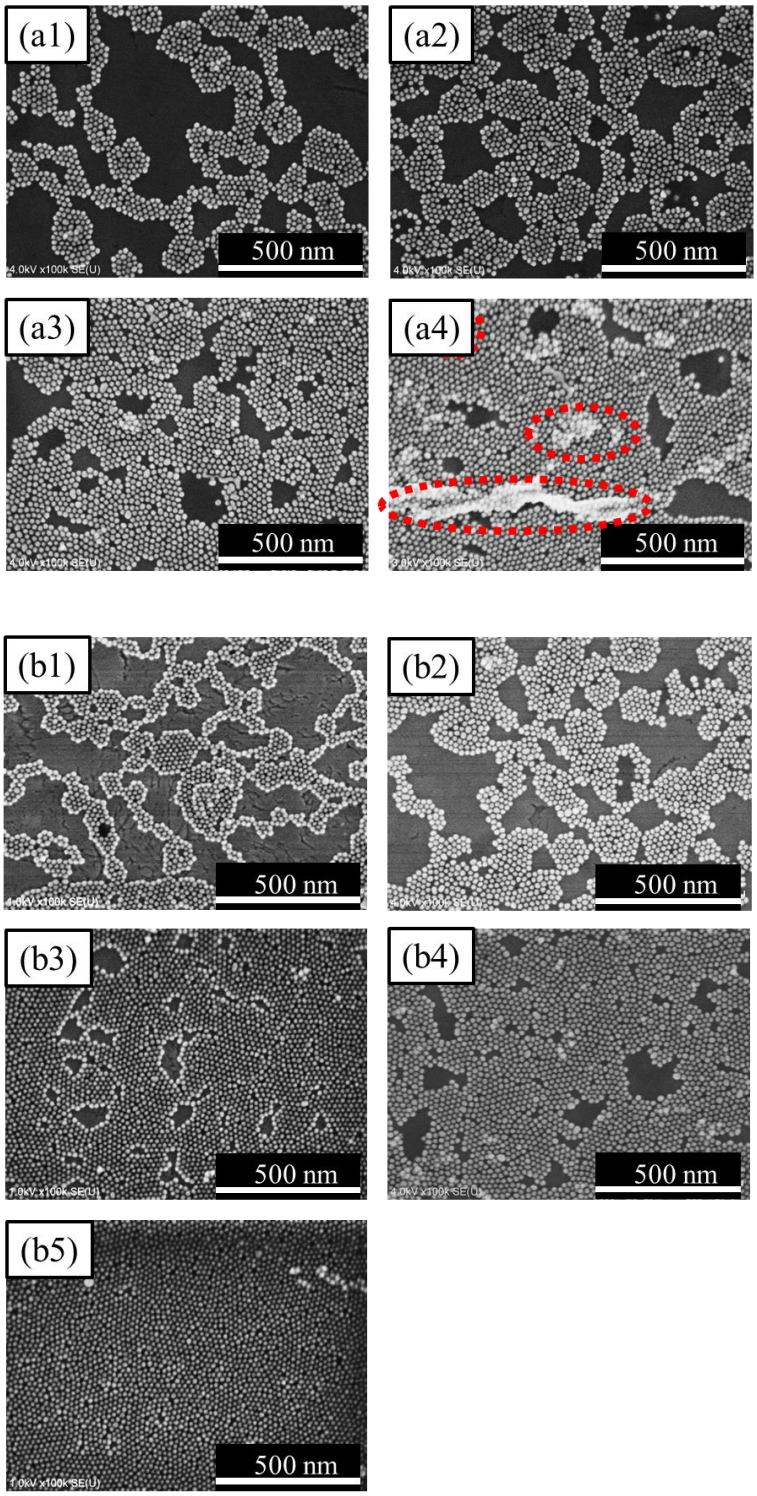

Figure 3. SEM images of LB films of ODT-AuNP (d = 17 nm) without PEG transferred onto ITO substrates at (a1) 7, (a2) 14, (a3) 25, and (a4) 38 mN m^{-1}, and of ODT-AuNP with PEG at (b1) 7, (b2) 14, (b3) 25, (b4) 38, and (b5) 45 mN m^{-1}. Red circles in (a4) showing the collapse of ODT-AuNP layer.

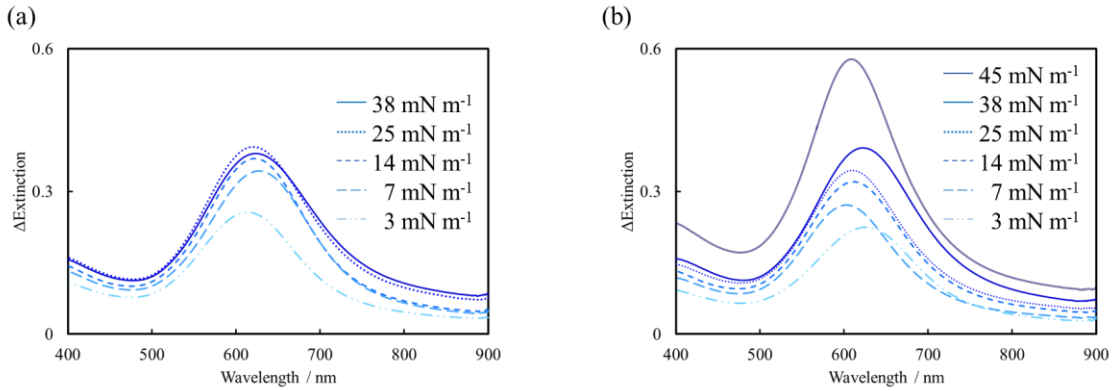

Figure 4. Extinction spectra of ODT-AuNP (d = 17 nm) films (a) without PEG and (b) with PEG transferred onto ITO substrates at various surface pressures.

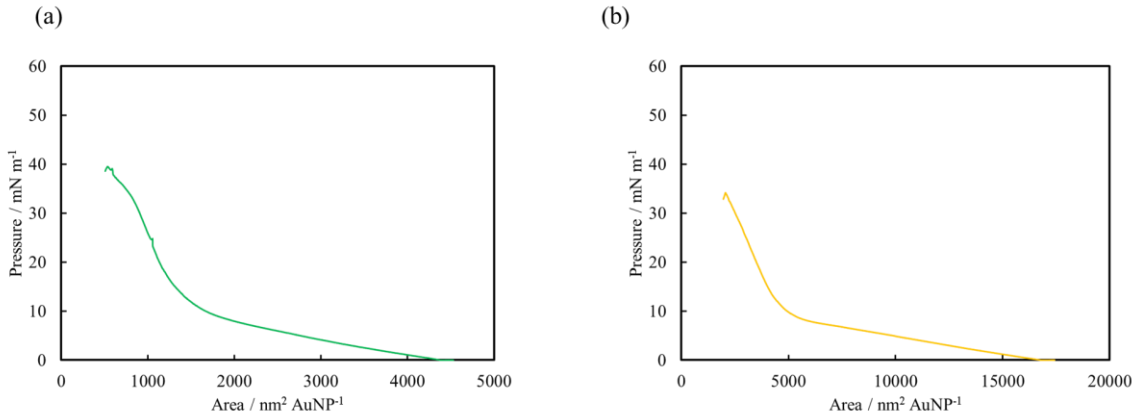

Figure 5. Surface pressure (π)-Area (A) isotherms of ODT-AuNPs with the diameters of (a) 28 and (b) 48 nm with PEG.

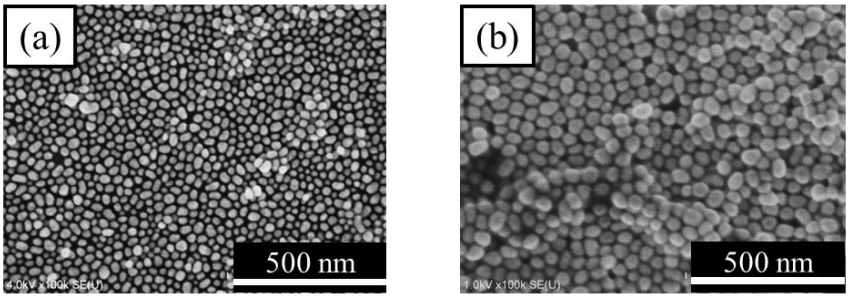

Figure 6. SEM images of LB films of ODT-AuNP with PEG transferred on the ITO substrate at (a) 36 mN m^{-1} (d = 28 nm) and (b) 31 mN m^{-1} (d = 48 nm).

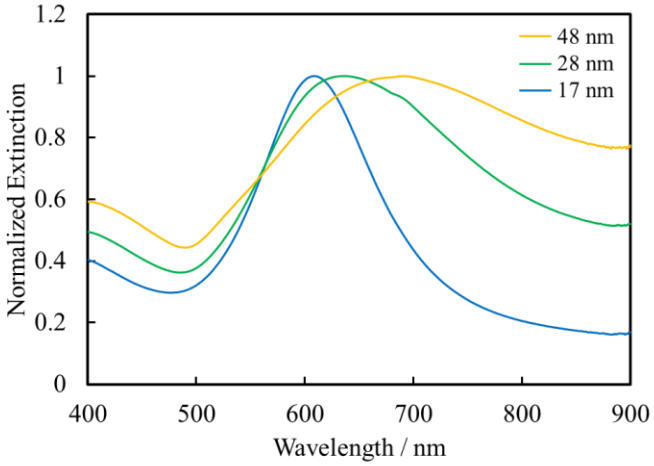

Figure 7. Extinction spectra of the ODT-AuNP films with the diameters of (a) 17 (blue), (b) 28 (green), and (c) 48 nm (yellow).

Displayed equation can be inserted where desired making sure it is assigned Word Style "Normal". Displayed equations can only be one column wide. If the artwork needs to be two columns wide, it must be relabeled as a figure, chart, or scheme and mentioned as such in the text.

$$K_s = -A\left(\frac{d\pi}{dA}\right) \quad (1)$$

ASSOCIATED CONTENT

Supporting Information.

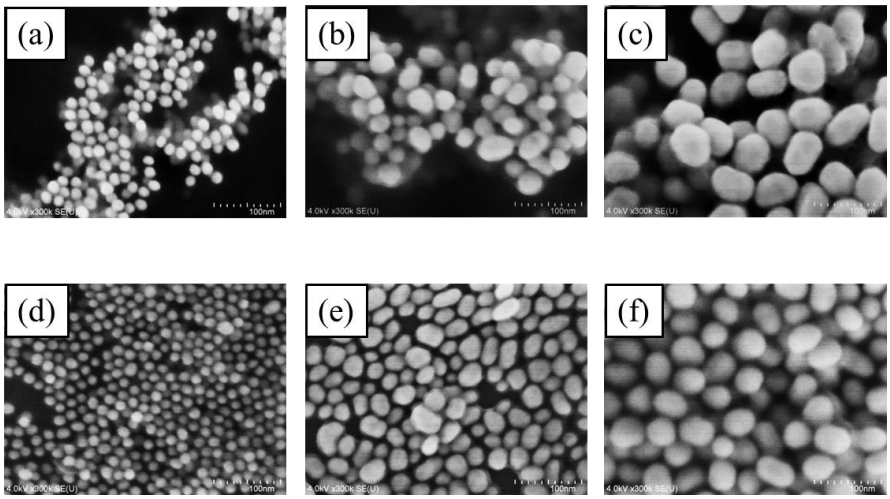

Figure S1. TEM images of cit-AuNPs with the diameters of (a) 17, (b) 28, and (c) 48 nm and ODT-AuNPs with the diameters of (d) 17, (e) 28, and (f) 48 nm.

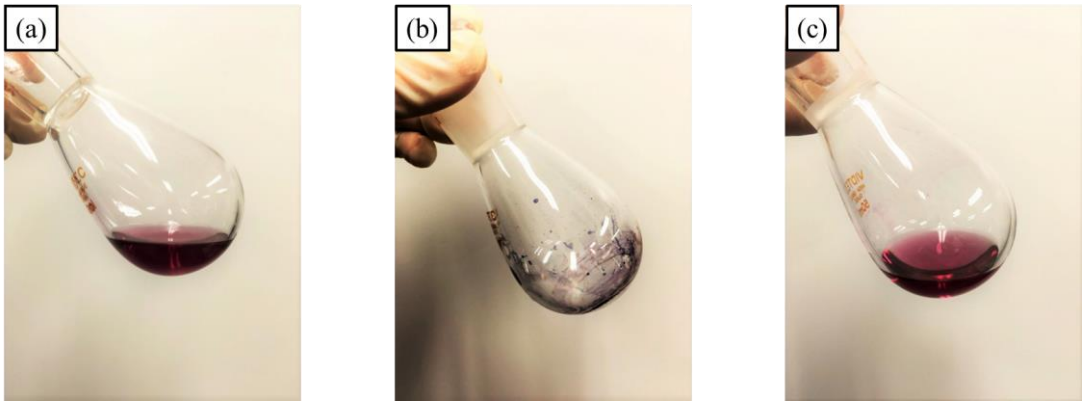

Figure S2. Photographs of ODT-AuNP/$CHCl_3$ (d = 17 nm) in a flask (a) before and (b) after drying, and (c) re-dispersion in chloroform.

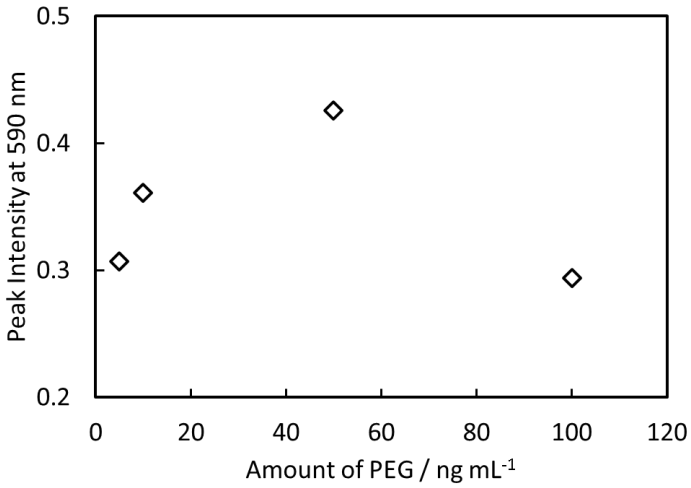

Figure S3. The dependency of the LSPR peak intensity at 590 nm on the additive amount of PEG.

In order to fabricate closely-packed 2D array, the dependent peak intensity on the amount of PEG was investigated. When the amount was 50 ng mL^{-1}, the peak intensity was maximum. This result indicates that the particle layer was most closely-packed by adding PEG of 50 ng mL^{-1} in this case.

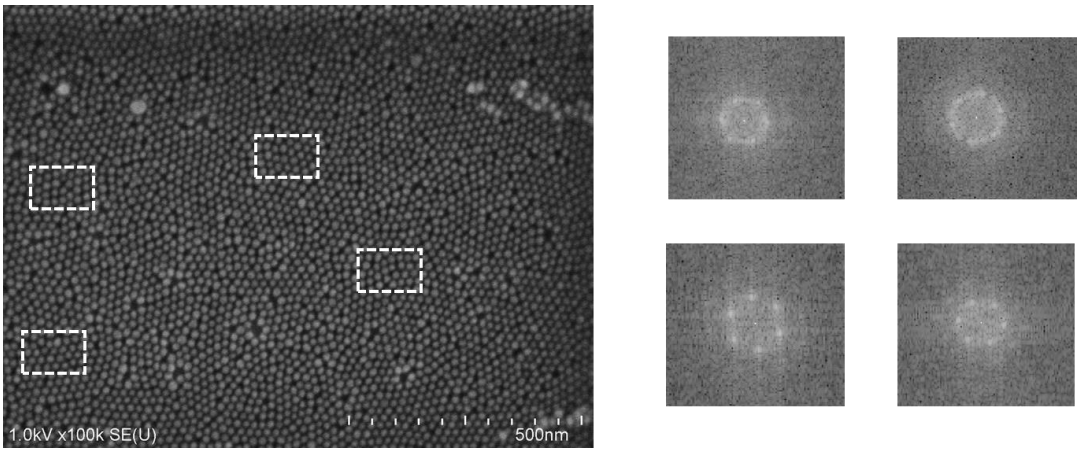

Figure S4. SEM and FFT images of 2D array of ODT-AuNPs (d = 17 nm) transferred onto an ITO substrate at 45 mN m^{-1}.

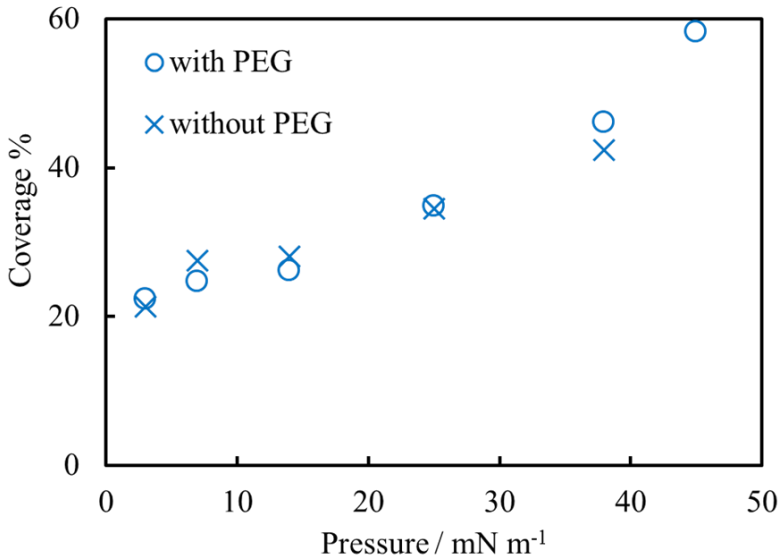

Figure S5. Coverages of ODT-AuNP (d = 17 nm) films without PEG (×) and with PEG (○) plotted against surface pressure.

AUTHOR INFORMATION

Corresponding Author

*E-mail: yukina@mail.cstm.kyushu-u.ac.jp and yamada@mail.cstm.kyushu-u.ac.jp

Present Addresses

Takuya Ishida, †Institute of Industrial Science, the University of Tokyo, 4-6-1 Komaba, Meguro-ku, Tokyo 153-8505, Japan

ACKNOWLEDGMENT

This work was supported by the Grants-in-Aid for JSPS Fellows Grant Number 13J11083 (for Ishida) and for Young Scientists (A) Grant Number 16H06120 (for Takahashi) from JSPS, Izumi Science and Technology Foundation (for Takahashi), and the research grant of the Noguchi Institute (for Takahashi).

REFERENCES

1. J. Takahara, S. Yamagishi, H. Taki, A. Morimoto, T. Kobayashi, Opt. Lett. 22 (1997) 475-477.
2. D. K. Gramotnev, S. I. Bozhevolnyi, Nature Photonics 4 (2010) 83-91.
3. V. Myroshnychenko, J. Rodríguez-Fernández, I. Pastoriza-Santos, A. M. Funston, C. Novo, P. Mulvaney, L. M. Liz-Marzánb, J. García de Abajo, Chem. Soc. Rev. 37 (2008) 1792-1805.
4. C. Deeb, X. Zhou, J. Plain, G. P. Wiederrecht, R. Bachelot, J. Phys. Chem. C 117 (2013) 10669-10676.
5. P. Anger, P. Bharadwaj, L. Novotny, Phys. Rev. Lett. 96 (2006) 113002.
6. K. Aslan, M. Wu, J. R. Lakowicz, C. D. Geddes, J. Am. Chem. Soc. 129 (2007) 1524-1525.
7. R. Matsumoto, H. Yonemura, S. Yamada, J. Phys. Chem. C 117 (2013) 2486-2493.
8. T. D. Neal, K. Okamoto, A. Scherer, M. S. Liu, A. K.-Y. Jen, Appl. Phys. Lett. 89 (2006) 221106.
9. G. M. Akselrod, C. Argyropoulos, T. B. Hoang, C. Ciracì, C. Fang, J. Huang, D. R. Smith, M. H. Mikkelsen, Nature Photonics 8 (2014) 835-840.
10. N. Terasaki, S. Nitahara, T. Akiyama, S. Yamada, Jpn. J. Appl. Phys. 44 (2005) 2795-2798.
11. T. Akiyama, M. Nakada, N. Terasaki, S. Yamada, Chem. Commun. (2006) 395-397.
12. K. Sugawa, T. Akiyama, H. Kawazumi, S. Yamada, Langmuir 25 (2009) 3887-3893.

13. T. Akiyama, K. Aiba, K. Hoashi, M. Wang, K. Sugawa, S. Yamada, Chem. Commun. 46 (2010) 306-308.

14. T. Kawawaki, Y. Takahashia, T. Tatsuma, Nanoscale 3 (2011) 2865-2867.

15. Y. Takahashi, S. Taura, T. Akiyama, S. Yamada, Langmuir 28 (2012) 9155-9160.

16. K. Leonard, Y. Takahashi, J. You, H. Yonemura, J. Kurawaki, S. Yamada, Chem. Phys. Lett. 584 (2013) 130-134.

17. J. You, K. Leonard, Y. Takahashi, H. Yonemura, S. Yamada, Phys. Chem. Chem. Phys. 16 (2014) 1166-1173.

18. K. A. Willets, R. P. V. Duyne, Annu. Rev. Phys. Chem. 58 (2007) 267-297.

19. Y. Takahashi, N. Miyahara, S. Yamada, Anal. Sci. 29 (2013) 101-105.

20. Y. Takahashi, K. Suga, T. Ishida, S. Yamada, Anal. Sci. 32 (2016) 275-280.

21. S. Rana, A. Bajaj, R. Mout, V. M. Rotello, Adv. Drug Deliv. Rev. 64 (2012) 200-216.

22. R. A. Sperling, P. Gil, F. Zhang, M. Zanella, W. J. Parak, Chem. Soc. Rev. 37 (2008) 1896-1908.

23. C. D. Walkey, J. B. Olsen, H. Guo, A. Emili, W. C. W. Chan, J. Am. Chem. Soc. 134 (2012) 2139-2147.

24. M. Brust, M. Walker, D. Bethell, D. J. Schiffrin, R. Whyman, J. Chem. Soc., Chem. Commun. (1994) 801-802.

25. C. K. Yee, R. Jordan, A. Ulman, H. White, A. King, M. Rafailovich, J. Sokolov, Langmuir 15 (1999) 3486-3491.

26. T. Yonezawa, K. Yasui, N. Kimizuka, Langmuir 17 (2001) 271-273.

27. H. J. Baika, S. Honga, S. Park, J. Coll. Interf. Sci. 358 (2011) 317-322.

28. T. Ishida, Y. Takahashi, H. Okamura, J. Kurawaki, S. Yamada, Vib. Spec. 73 (2014) 10-14.

29. T. Ishida, Y. Tachikiri, Y. Takahashi, S. Yamada, Trans. Mat. Res. Soc. Japan 40 (2015) 253-256.

30. P. Peumans, A. Yakimov, S. R. Forrest, J. Appl. Phys. 93 (2003) 3693-3723.

31. B. P. Rand, P. Peumans, S. R. Forrest, J. Appl. Phys. 96 (2004) 7519-7526.

32. S. S. Kim, S. I. Na, J. Jo, D. Y. Kim, Y. C. Nah, Appl. Phys. Lett. 93 (2008) 073307.

33. K. Okamoto, I. Niki, A. Shvartser, Y. Narukawa, T. Mukai, A. Scherer, Nature Mater. 3 (2004) 601-605.

34. J. S. Biteen, D. Pacifici, N. S. Lewis, H. A. Atwater, Nano Lett. 5 (2005) 1768-1773.

35. X. Xu, M. Funato, Y. Kawakami, K. Okamoto, K. Tamada, Opt. Express 21 (2013) 3145-3151.

36. R. Elghanian, J. J. Storhoff, R. C. Mucic, R. L. Letsinger, C. A. Mirkin, Science 277 (1997) 1078-1081.

37. M. Toma, K. Toma, K. Michioka, Y. Ikezoe, D. Obara, K. Okamoto, K. Tamada, Phys. Chem. Chem. Phys. 13 (2011) 7459-7466.

38. K. Ueno, S. Juodkazis, T. Shibuya, Y. Yokota, V. Mizeikis, K. Sasaki, H. Misawa, J. Am. Chem. Soc. 130 (2008) 6928-6929.

39. Y. Nishijima, K. Ueno, Y. Yokota, K. Murakoshi, H. Misawa, J. Phys. Chem. Lett. 1 (2010) 2031-2036.

40. T. Karakouz, D. Holder, M. Goomanovsky, A. Vaskevich, I. Rubinstein, Chem. Mater., 21 (2009) 5875-5885.

41. T. Ochiai, K. Isozaki, F. Pincella, T. Taguchi, K. Nittoh, K. Miki, Appl. Phys. Express 6 (2013) 102001.

42. F. Pincella, K. Isozaki, K. Miki, Light: Science & Applications 3 (2014) e133.

43. J. Schmitt, G. Decher, W. J. Dressick, S. L. Brandow, R. E. Geer, R. Shashidhar, J. M. Calvert, Adv. Mater. 9 (1997) 61-65.

44. T. Yonezawa, S. Onoue, T. Kunitake, Adv. Mater. 10 (1998) 414-416.

45. N. Chandrasekharan, P. V. Kamat, Nano Lett. 1 (2001) 67-70.

46. M. Suzuki, Y. Niidome, N. Terasaki, K. Inoue, Y. Kuwahara, S. Yamada, Jpn. J. Appl. Phys. 43 (2004) L554-L556.

47. F. Reincke, S. G. Hickey, W. K. Kegel, D. Vanmaekelbergh, Angew. Chem. Int. Ed. 116 (2004) 464-468.

48. B. Kim, M. A. Carignano, S. L. Tripp, A. Wei, Langmuir 20 (2004) 9360-9365.

49. N. A. Kotov, F C. Meldrum, C. Wu, J. H. Fendler, J. Phys. Chem. 98 (1994) 2735-2738.

50. N. A. Kotov, F. C. Meldrum, C. Wu, J. H. Fendler, J. Phys. Chem. 98 (1994) 8827-8830.

51. S. Huang, G. Tsutsui, H. Sakaue, S. Shingubara, T. Takahagi, J. Vac. Sci. Technol. B 19 (2001) 115-120.

52. S. Huang, K. Minami, H. Sakaue, S. Shingubara, T. Takahagi, Langmuir 20 (2004) 2274-2276.

53. V. Aleksandrovic, D. Greshnykh, I. Randjelovic, A. Fromsdorf, A. Kornowski, S. V. Roth, C. Klinke, H. Weller, ACS Nano 2 (2008) 1123-1130.

54. C. Y. Lau, H. Duan, F. Wang, C. B. He, H. Y. Low, J. K. W. Yang, Langmuir 27 (2011) 3355-3360.

55. C.-L. Hsu, K.-H. Wang, C.-H. Chang, W.-P. Hsu, Y.-L. Lee, Appl. Surf. Sci. 257 (2011) 2756-2763.

56. A. Yoshida, K. Imazu, X. Li, K. Okamoto, K. Tamada, Langmuir 28 (2012) 17153-17158.

57. K. Okamoto, B. Lin, K. Imazu, A. Yoshida, K. Toma, M. Toma, K. Tamada, Plasmonics 8 (2013) 581-590.

58. M. Mukhopadhyay, S. Hazra, RSC Adv. 6 (2016) 12326-12336.

59. K. Vegso, P. Siffalovic, E. Majkova, M. Jergel, M. Benkovicova, T. Kocsis, M. Weis, S. Luby, K. Nygård, O. Konovalov, Langmuir 28 (2012) 10409-10414.

60. R. K. Gupta, K. A. Suresh, S. Kumar, Phys. Rev. E 78 (2008) 032601.

61. S. Kubowicz, M. A. Hartmann, J. Daillant, M. K. Sanyal, V. V. Agrawal, C. Blot, O. Konovalov, H. Möhwald, Langmuir 25 (2009) 952-958.

62. C. Tira, D. Tira, T. Simon, S. Astilean, J. Mol. Struct. 1072 (2014) 137-143.

Insert Table of Contents Graphic and Synopsis Here

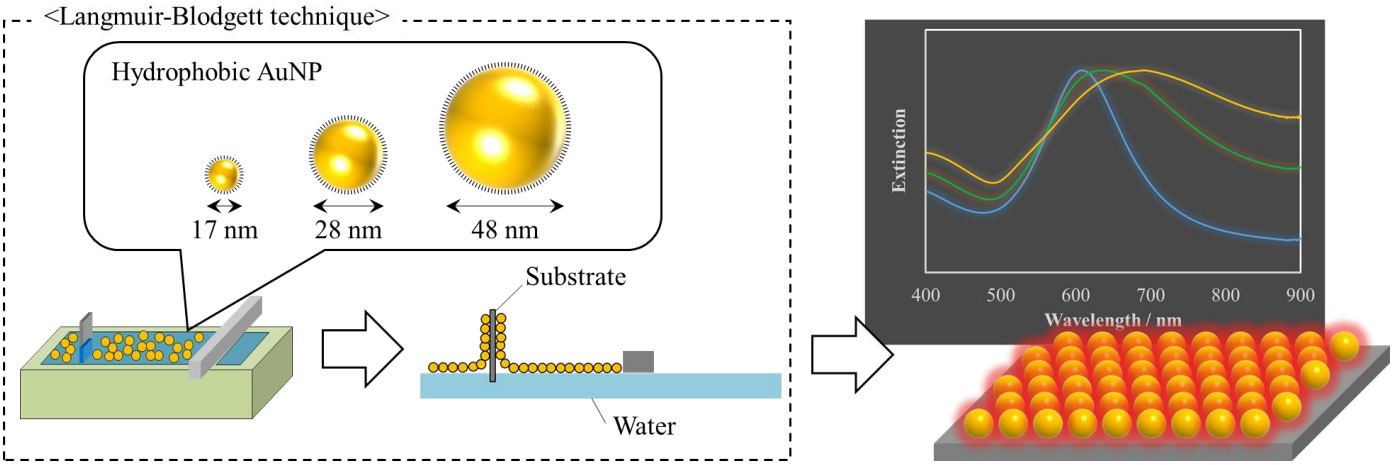

Highlights

- Hydrophobic gold nanoparticles (AuNPs) by our method were large and stable enough.
- Two-dimensional (2D) arrays of the AuNPs were obtained by Langmuir-Blodgett method with polyethylene glycol.
- The plasmon resonant wavelength of the 2D arrays can be controlled by the diameter.